Electronic structure of Li_xCoO_2 studied by photoemission spectroscopy and unrestricted Hartree-Fock calculations

K. Ikedo, Y. Wakisaka, and T. Mizokawa
Department of Physics and Department of Complexity Science and Engineering, University of Tokyo, Chiba 277-8561, Japan

C. Iwai, K. Miyoshi, and J. Takeuchi
Department of Material Science, Shimane University, Matsue 690-8504, Japan

(Received 1 March 2010; revised manuscript received 23 June 2010; published 13 August 2010)

We report on an electronic structural study of Li_xCoO_2 single crystals (x=0.99, 0.71, 0.66, and 0.46) which have hole-doped CoO_2 triangular lattices. The valence-band photoemission spectra show that the Fermi level is located near the top of the Co 3d t_{2g} bands and that, by the reduction in x, the Co 3d t_{2g} peak is shifted to the lower binding-energy side. This energy shift is consistent with the chemical-potential shift by the hole doping to the t_{2g} bands. The fine structures near the Fermi level indicate the splitting of the t_{2g} bands into the a_{1g} and e_g' components. The electronic structure parameters such as the charge-transfer energy Δ are obtained by the cluster-model analysis of the Co 2p core-level spectra. The unrestricted Hartree-Fock calculation using the obtained parameter values predicts that the doped holes are accommodated by the a_{1g} band up to the doping level x of 0.46 which is consistent with the observation in the valence-band spectra. However, the valence-band spectra cannot be reproduced by the unrestricted Hartree-Fock calculation indicating that the correlation effect from the electron-electron and electron-phonon interactions is substantial in Li_xCoO_2.

DOI: 10.1103/PhysRevB.82.075126 PACS number(s): 71.28.+d, 79.60.−i

I. INTRODUCTION

Layered cobaltes with CoO_2 planes, in which Co ions form two-dimensional triangular lattices with edge-sharing CoO_6 octahedra, are known as cathode materials for rechargeable batteries, large thermoelectric materials, and superconductors. Among them, Li_xCoO_2 has been widely studied for the practical use as a positive electrode material in commercial Li ion batteries.[1] Rechargeable batteries using Li_xCoO_2 cathods exhibit the highest performance among batteries using similar transition-metal oxides.[1–4] Li_xCoO_2 with the layered α-$NaFeO_2$ structure belongs to the rhombohedral system (space group $R\bar{3}m$) and has the CoO_2 layers and the interlayers of Li ions which are alternating stacked along the c axis.[5] The Li ions occupy the octahedral sites between the CoO_2 layers. On the other hand, Na_xCoO_2 has a similar structure with different staking sequence of oxygen atom layers, where the Na ions occupy the prismatic sites with two CoO_2 sheets per unit cell. Na_xCoO_2 has been intensively investigated originally due to good thermoelectric properties[6–8] and recently due to the superconductivity in the hydrated compound $Na_{0.35}CoO_2 \cdot 1.3H_2O$ below $T_c \sim 5$ K.[9] Indeed, Na_xCoO_2 has been found to exhibit various interesting low temperature properties with changing Na content x, such as metal-insulator transition (x=0.5),[10] heavy-mass Fermi-liquid behavior ($x \sim 0.75$),[11] and spin-density wave (SDW) state ($x \geq 0.75$).[12]

X-ray absorption spectroscopy (XAS) studies[13,14] and angle-resolved photoemission spectroscopy studies[15–17] on the hole-doped CoO_2 triangular lattices revealed that both Co^{3+} and Co^{4+} commonly have the low-spin configuration (t_{2g}^6 and t_{2g}^5, respectively) at low temperatures. The triply degenerate t_{2g} states are further split into the a_{1g} and e_g' states due to the trigonal ligand field. By changing the angle between the x-ray polarization vector and the surface normal (c axis), the angular dependence of the XAS intensity was observed which gives information about the hole distribution between the a_{1g} and e_g' orbitals. However, it is still controversial whether the e_g' orbitals accommodate the doped holes in superconducting Na_xCoO_2 or not. Compared with Na_xCoO_2, the electronic structure of Li_xCoO_2 has not been studied well although it is widely used in commercial Li ion batteries. For better understanding of the electronic properties of Li_xCoO_2 as well as Na_xCoO_2, it is worthy to investigate the electronic structure of Li_xCoO_2 and compare it with that of Na_xCoO_2.

For stoichiometric $LiCoO_2$, magnetic-susceptibility (χ) measurements,[18] x-ray photoelectron spectroscopy (XPS) analysis,[19] and band-structural calculations[20] indicate that Co^{3+} ions are in the low-spin state (t_{2g}^6) with S=0 at ambient temperature. χ and NMR experiments down to 4.2 K (Ref. 21) confirmed that $LiCoO_2$ does not exhibit any magnetic transitions at low temperatures. Although $LiCoO_2$ is known to be an insulator, Li deficient Li_xCoO_2 for $0.5 < x < 1$, in which Li ions are removed/deintercalated by an electrochemical reaction similar to that in Li ion batteries, exhibits metallic behavior. An insulator-to-metal transition was found at around x=0.95 by resistivity (ρ) measurements. The value of ρ at 275 K gradually decreases with further lowering x.[22] Hertz *et al.*[23] show that the low-temperature specific-heat data for Li_xCoO_2 samples are well explained by the hole doping in the triply degenerate t_{2g} states with decreasing x because Li deintercalation increases the Co valence, i.e., the population of Co^{4+} ions. Considering that ρ was measured using polycrystalline samples, the transport properties of $Li_{0.7}CoO_2$ seem to be almost comparable to those of $Na_{0.7}CoO_2$, which is known to be a good thermoelectric material.[9,24,25]

As for the magnetic properties of the doped systems, in Na_xCoO_2 with $x \geq 0.75$, a long-range magnetic order, which

is clearly incommensurate SDW in single crystalline samples, was found at low temperatures by positive muon spin rotation and relaxation (μ^+SR) experiments.[26,27] The existence of long-range magnetic order in Na_xCoO_2 was reconfirmed later by not only μ^+SR (Ref. 28) but also neutron-diffraction experiments.[29] On the other hand, magnetic properties of Li_xCoO_2 are not fully understood yet. The magnetism of Li_xCoO_2 polycrystalline samples with $0.1 \leq x \leq 1$ has been investigated by μ^+SR and χ measurements.[30,31] Mukai *et al.*[31] show the temperature dependence of χ for Li_xCoO_2 with $x \geq 0.1$. For $LiCoO_2$, the $\chi(T)$ curve increases very slowly with decreasing temperature down to ~50 K and then increases more rapidly below 50 K, indicating the appearance of localized moments. For Li_xCoO_2 with $0.49 \leq x \leq 0.75$, χ increases linearly but slowly down to ~175 K ($=T_m$) then suddenly drops at T_m and reaches a broad minimum at ~100 K, and finally χ increases with further decreasing T. For Li_xCoO_2 with $x \leq 0.44$, T_m disappears from the $\chi(T)$ curve, and it also exhibits a Pauli-paramagnetic behavior down to ~100 K for $x=0.44$ and down to ~50 K for $x=0.1$. These results indicate that the spin state of Co^{4+} ions may change from the high-temperature high-spin state ($t_{2g}^3 e_g^2$, $S=5/2$) to the low-temperature low-spin state (t_{2g}^5, $S=1/2$) or the mixture of low-spin and intermediate-spin ($t_{2g}^4 e_g^1$, $S=3/2$) states. In addition, $\chi(T)$ has been measured for Li_xCoO_2 ($x=0.92$, 0.47, and 0.42) using single crystalline samples.[32] It has been found that, both for $x=0.47$ and 0.42, the $\chi(T)$ curve exhibits a sudden drop at $T_m \sim 170$ K, suggesting the occurrence of the spin state transition at T_m.

In this work, we have studied the electronic structure of Li_xCoO_2 single crystals with $x=0.99$, 0.71, 0.66, and 0.46 using XPS, ultraviolet photoemission spectroscopy (UPS), and subsequent model calculations. The XPS results provide important pieces of information to understand the interesting magnetic properties of Li_xCoO_2. The UPS results show a systematic evolution of electronic states as a function of hole concentration x. The present photoemission study has revealed the electronic structure of Li_xCoO_2 which is the basis of the Li ion battery and is useful for more systematic understanding of hole-doped CoO_2 triangular lattices.

II. EXPERIMENT AND CALCULATION

Single crystals of Li_xCoO_2 with $x=0.99$, 0.71, 0.66, and 0.46 were prepared as reported by Miyoshi *et al.*[32,33] The XPS measurements were performed using a JPS-9200 spectrometer equipped with a monochromatized Al $K\alpha$ x-ray source ($h\nu=1486.6$ eV) at 300 and 20 K. The total-energy resolution was 0.6 eV. The binding energy was calibrated using gold reference samples with the Au $4f_{7/2}$ peak at 84.0 eV. The UPS data were taken using a SES-100 spectrometer with a He I source ($h\nu=21.2$ eV) at 20 K. The total-energy resolution was 30 meV. The binding energy was calibrated using the Fermi edge of gold reference samples. The base pressure of the spectrometer was in the 10^{-7} Pa range. The single crystals were cleaved *in situ* in order to obtain clean surfaces.

The density of states (DOS) and the band dispersions considering the CoO_2 layers were calculated by the unrestricted

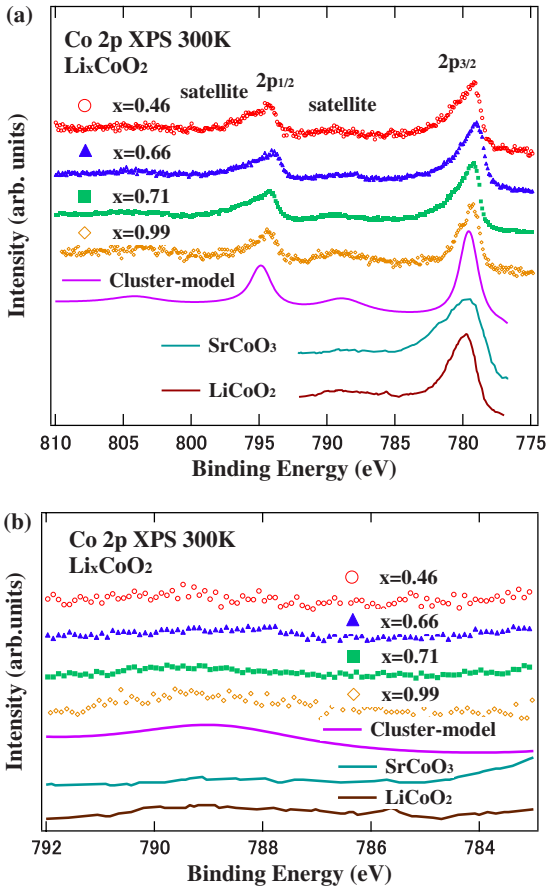

FIG. 1. (Color online) (a) Co $2p$ XPS spectra of Li_xCoO_2 ($x=0.99$, 0.71, 0.66, and 0.46) taken at 300 K. The three solid curves indicate the result of the cluster-model calculation, the reference spectra of $SrCo^{4+}O_3$ (Ref. 38) and $LiCo^{3+}O_2$ (Ref. 19), respectively. (b) The closeup of the satellite region.

Hartree-Fock approach with the d-p Hamiltonian.[34] Various parameters were determined by the cluster-model calculation of the Co $2p$ XPS spectra of the same samples. Δ, U, and $(pd\sigma)$ were found to be 1.0 eV, 6.5 eV, and −2.2 eV, respectively. Here, the ratio $(pd\sigma)/(pd\pi)$ is −2.16. Remaining transfer integrals expressed by $(pp\sigma)$, $(pp\pi)$, $(dd\sigma)$, and $(dd\pi)$ are fixes at −0.6 eV, 0.15 eV, −0.3 eV, and 0.15 eV, respectively, for the undistorted lattice with the regular CoO_6 octahedron. When the lattice is distorted, the transfer integrals are scaled using Harrison's law. Here Δ denotes the charge-transfer energy for Co^{3+} or specifically $\Delta=\epsilon_d-\epsilon_p+6U$. From a detailed structural report,[23] the average Co-Co and Co-O distances in the triangular lattice layers of Li_xCoO_2 are estimated as 2.82 Å and 1.92 Å, respectively, which correspond to the ratio R of 0.89 (meaning that the CoO_6 octahedron is compressed along the c axis with keeping its Co-Co distance until its thickness reaches 89% from its original one).

III. RESULTS AND DISCUSSION

Figures 1 and 2 show the Co $2p$ XPS spectra of Li_xCoO_2 ($x=0.99$, 0.71, 0.66, and 0.46) taken at 300 K and 20 K,

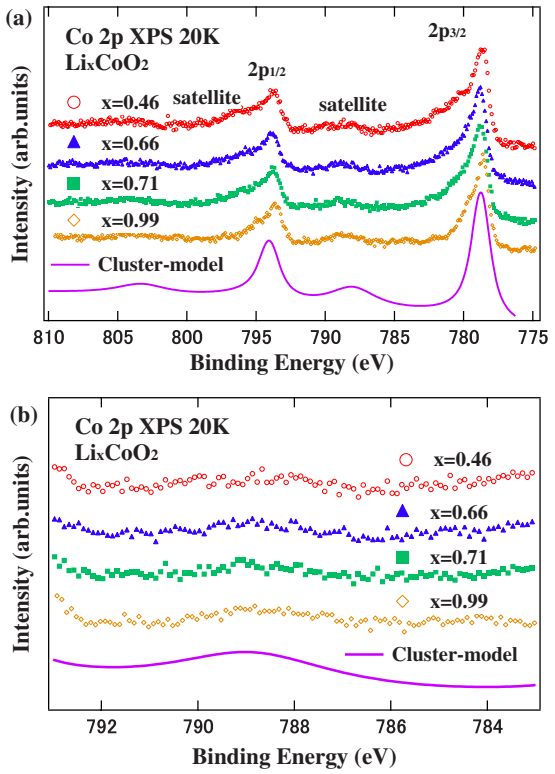

FIG. 2. (Color online) (a) Co $2p$ XPS spectra of Li_xCoO_2 (x =0.99, 0.71, 0.66, and 0.46) taken at 20 K. The solid curve indicates the result of the cluster-model calculation. (b) The closeup of the satellite region.

respectively. Basically, the line shape of the Co $2p$ spectra is consistent with the low-spin configurations.[18–20] Both at 300 and 20 K, the main peaks of the Co $2p_{3/2}$ and Co $2p_{1/2}$ spectra become broader with decreasing x due to the tailing on the higher binding-energy side. The tailing of the main peak is related to the Co^{3+}/Co^{4+} mixed-valence nature and/or the metallic nature of the ground state. The recent study on the magnetic and electronic properties of Li_xCoO_2 strongly indicates that the Co^{3+}/Co^{4+} ordering and the metallic behavior coexist below $T_S \sim 155$ K.[33] Even above the Co^{3+}/Co^{4+} ordering temperature, the Co sites can have short-range correlation of Co^{3+}/Co^{4+} mixed valence. In the mixed-valence picture, the tailing of the main peak at 20 and 300 K can be attributed to the Co^{4+} component with the binding energy higher than the Co^{3+} component. This picture is consistent with the fact that the tailing effect increases with decreasing Li content x. In addition, the core-hole screening effect due to the metallic component can contribute to the tailing of the main peak. Probably, in the present Li_xCoO_2, both the metallic state and the Co^{4+} component contribute to the tailing of the Co $2p$ main peaks.

The intensity and the position of the charge-transfer satellite for x=0.99 can be analyzed by the configuration-interaction calculation on the CoO_6 cluster model. Here, we assume that the Co $2p$ spectrum for x=0.99 is dominated by the low-spin Co^{3+} contribution. With Δ=1.0 eV, U =6.5 eV, and $(pd\sigma)$=−2.2 eV, the calculated spectrum can explain the energy position and the intensity of the satellite structure as shown in Figs. 1 and 2. Although the Co $2p_{3/2}$ and Co $2p_{1/2}$ main peaks can be affected by the long-range screening process beyond the CoO_6 cluster[35] that is not included in the present single-site cluster model calculation, the overall Co $2p$ spectrum is well reproduced by the calculation except the line shape of the main peaks. Therefore, Δ, U, and $(pd\sigma)$ obtained by the single-site cluster-model analysis are reliable as shown in various transition-metal oxides.[36,37]

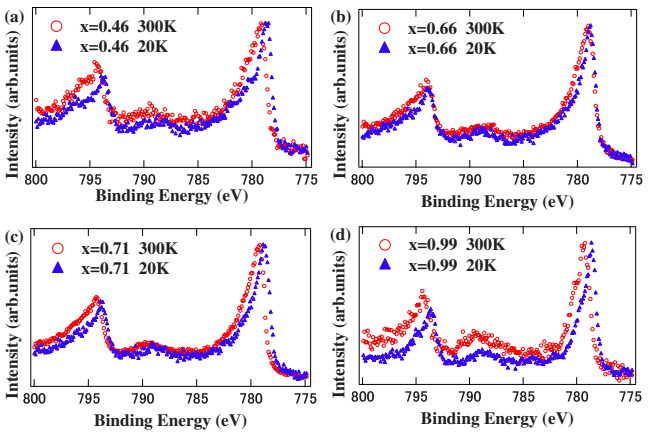

FIG. 3. (Color online) Co $2p$ XPS spectra of Li_xCoO_2 taken at 300 and 20 K for (a) x=0.99, (b) 0.71, (c) 0.66, and (d) 0.46.

Since the charge-transfer satellite is given by the local charge-transfer screening process within the CoO_6 cluster, the energy position, and the intensity of the satellite for the Co^{3+} component are expected to be insensitive to the Li content x. Actually, at 20 K, the energy position and the intensity of the satellite do not change appreciably with x. However, the binding energy of the satellite is slightly lowered with decreasing x. Since the satellite structure of $SrCo^{4+}O_3$ is very broad and is located at the lower binding-energy side of that in $LiCoO_2$,[19,38] this observation suggests that the satellite for the Co^{4+} component becomes important with decreasing x. Interestingly, at 300 K, the binding energy of the satellite is lowered in going from x=0.99 to x=0.66 and then increased from x=0.66 to x=0.46, suggesting that, even at 300 K, the Co^{4+} state tends to be stabilized due to commensurate charge ordering expected for x=0.66. The temperature dependence of the Co $2p$ spectra for x=0.99, 0.71, 0.66, and 0.46 are displayed in Fig. 3. The Co $2p$ peaks of x=0.99, 0.71, and 0.46 are shifted to the higher binding-energy side with increasing temperature, which is consistent with the upward chemical-potential shift expected for metals with p-type carriers. Interestingly, the energy shift between 20 and 300 K is suppressed at x=0.66. This observation can be related to stability of the Co^{3+}/Co^{4+} charge ordering at x=0.66. In addition, the line shape of the main peak has strong temperature dependence in the heavily hole-doped sample with x=0.46, indicating that core-hole screening effect due to the metallic component becomes important at x=0.46.

Figure 4 shows the valence-band UPS spectra of Li_xCoO_2 taken at 20 K. The Co $3d$ t_{2g} peaks of Li_xCoO_2 with x =0.99, 0.71, 0.66, and 0.46 are observed in the binding energy range from 0.5 to 1.5 eV. With decreasing x, the position of the Co $3d$ t_{2g} peak is shifted to the lower binding-energy side. The energy shift of the t_{2g} peak as a function of

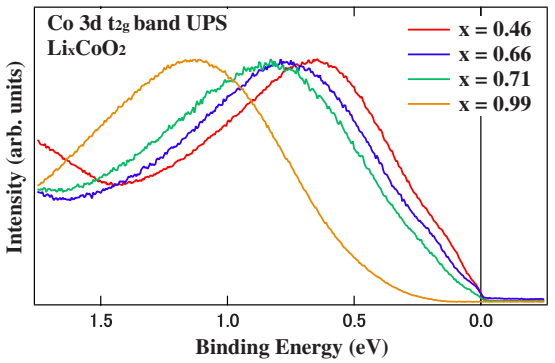

FIG. 4. (Color online) Valence-band UPS spectra of Li_xCoO_2 (x=0.99, 0.71, 0.66, and 0.46) at 20 K.

x can be assigned to the chemical-potential shift caused by the hole doping in the t_{2g} band. The chemical potential or the Fermi level is shifted to the higher binding-energy side with decreasing x which is consistent with the hole doping in the t_{2g} band.

Figure 5 shows the valence-band UPS spectra near the Fermi level of Li_xCoO_2 taken at 20 K. The valence band of $Li_{0.99}CoO_2$ does not reach the Fermi level, indicating that it is an insulator. On the other hand, the valence bands of $Li_{0.71}CoO_2$, $Li_{0.66}CoO_2$, and $Li_{0.46}CoO_2$ reach the Fermi levels, showing that they are metals. The shoulder at ~0.2 eV gradually moves to the Fermi level with decreasing x. It is possible to assign the shoulder to the e_g' bands which are split from the t_{2g} bands due to the trigonal ligand field. In this picture, the electronic states at the Fermi level are dominated by the a_{1g} band. The e_g' bands become closer to the Fermi level by the hole doping and emerge more clearly in the photoemission spectra with decreasing x. In case of Li_xCoO_2, the e_g' bands do not reach the Fermi level up to the doping level x of 0.46.

Figure 6 shows the band dispersion for x=0.99 (N_k =17.99) and x=0.46 (N_k=17.46) obtained from the unrestricted Hartree-Fock calculations using the parameters of the cluster-model analysis. Here, we have employed the multiband d-p model and performed the unrestricted Hartree-Fock calculations. N_k is the number of occupied states at each momentum point with k. As estimated from the cluster-model analysis of the Co 2p spectrum, Δ, U, and ($pd\sigma$) for Li_xCoO_2 are 1.0 eV, 6.5 eV, and −2.2 eV, respectively,

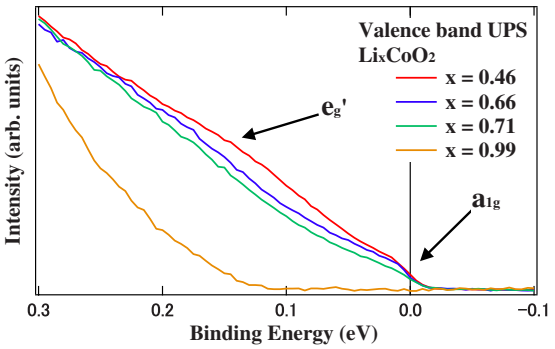

FIG. 5. (Color online) Valence-band UPS spectra of Li_xCoO_2 (x=0.99, 0.71, 0.66, and 0.46) near Fermi level at 20 K.

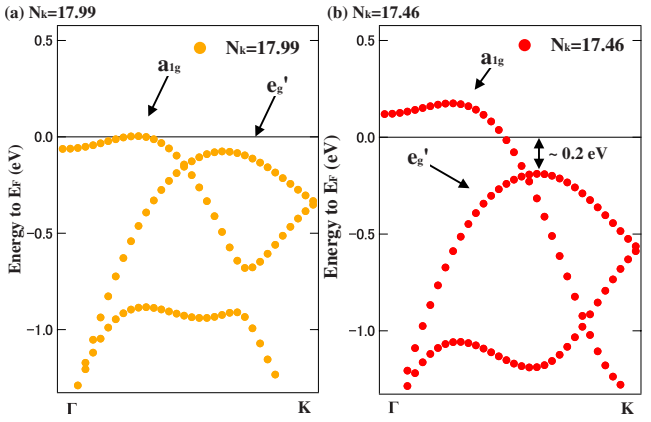

FIG. 6. (Color online) Band dispersions along the Γ-K directions for the hole-doped t_{2g} bands in the CoO_2 triangular lattice using unrestricted Hartree-Fock calculation for (a) N_k=17.99 and (b) N_k=17.46.

whose values are more or less consistent with the chemical trend obtained in various transition-metal compounds. For N_k=17.99, the Fermi level is located at the top of the a_{1g} band due to the 0.01 hole doping per Co. In going from N_k =17.99 to N_k=17.46, the a_{1g} band is shifted to the higher energy and more holes are accommodated by the a_{1g} band. Even for N_k=17.46, the top of the e_g' bands is still located at ~0.2 eV below the Fermi level, which is consistent with the UPS result for x=0.46. Similar trends are also reported for Na_xCoO_2.[39,40] Here, it should be pointed out that the avoided crossing is negligibly small for x=0.99 while it increases with decreasing x.[41]

In order to examine the positions of the a_{1g} and e_g' components in Li_xCoO_2, the valence-band UPS spectra are compared with the DOS calculated by the unrestricted Hartree-Fock method in Fig. 7. The calculated DOS is convoluted with a Lorentzian function with full width of half maximum of 50 meV. First, the experimental UPS spectra show single broad Co t_{2g} peaks in contrast to the calculated DOS with multiple sharp peaks. The broadening effects are probably due to the electron-electron and electron-phonon interactions

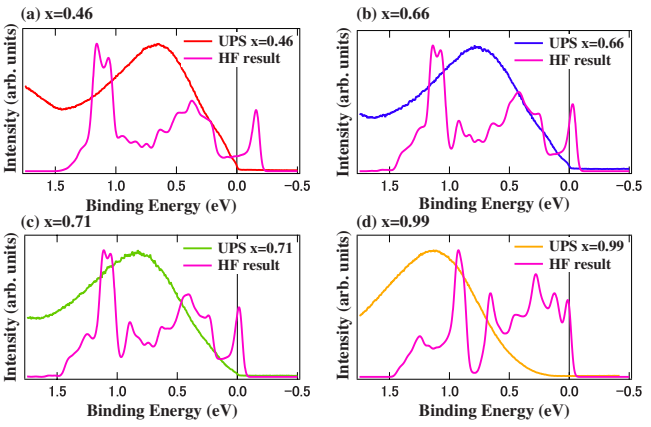

FIG. 7. (Color online) Valence-band UPS spectra of Li_xCoO_2 at 20 K compared with the calculated DOS for (a) x=0.46, (b) x =0.66, (c) x=0.71, and (d) x=0.99.

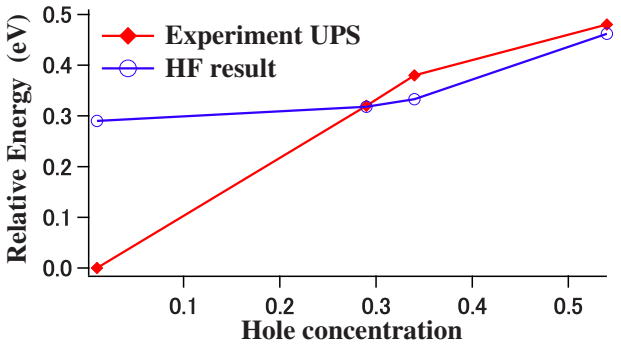

FIG. 8. (Color online) Chemical-potential shift $\Delta\mu$ as a function of hole concentration in the CoO_2 triangular lattice. The closed diamonds (open circles) indicate $\Delta\mu$ obtained from the experimental (calculated) results.

that are not considered in the calculation and would be important to reproduce the experimental results. Second, the experimental result for $x=0.99$ is shifted to the higher binding-energy side compared with the calculated DOS. The energy shift can be assigned to the strong electron-phonon interaction. The line shape of the t_{2g} bands for $x=0.99$ reminds us the polaronic effect in the photoemission spectrum which can be demonstrated in the simple model with a localized electron of energy interacting with Einstein phonons of frequency ω. In this picture, the Fermi level basically corresponds to the zero-phonon peak position and the main t_{2g} peak is located at $g\omega$ below the Fermi level, where g is the coupling constant and ω is the frequency of the phonon. At $x=0.99$, the spectral weight of the zero-phonon peak or the quasiparticle peak is negligibly small, indicating that the quasiparticle renormalization due to the electron-phonon coupling is very large. In addition to the main t_{2g} peak probably derived from the strong electron-phonon interaction, spectral features near the Fermi level are observed for $x=0.71$, 0.66, and 0.46 which correspond to the quasiparticle spectral weight. At $x=0.71$, 0.66, and 0.46, the quasiparticle spectral weight is still small compared to the main t_{2g} peak in the binding energy range from 0.5 to 1.5 eV. The position of a_{1g} and e_g' bands and the chemical-potential shift ($\Delta\mu$) with x for $x=0.71$, 0.66, and 0.46 are roughly reproduced by the unrestricted Hartree-Fock calculations. As for the position of a_{1g} and e_g' bands, the shoulder at the lower binding-energy side of Co $3d$ t_{2g} peak observed for $x=0.71$, 0.66, and 0.46 can be assigned to the e_g' bands located below the a_{1g} band as discussed in the previous paragraph. The splitting between the a_{1g} and e_g' bands is reproduced by the calculations for $x=0.71$, 0.66, and 0.46. Although the band shape depends on the doping level and the rigid-band condition is not exactly satisfied, the chemical-potential shift $\Delta\mu$ can be estimated from the energy shift of the a_{1g} peak. Figure 8 shows the comparison between the calculated $\Delta\mu$ and the observed $\Delta\mu$ determined from the energy shift of the t_{2g} peak. The $\Delta\mu$ as a function of x is almost consistent with that of the calculated result for $x\leq 0.71$. It is interesting that $\Delta\mu$ qualitatively agrees with the unrestricted Hartree-Fock result although the t_{2g} bands are likely to be strongly renormalized by the electron-phonon interaction in terms of the small quasiparticle spectral weight.

The electron-phonon coupling effect in the multiband system has been studied for Mn oxides.[42] In the insulating case ($x=0.99$), the quasiparticle spectral weight z for the a_{1g} and e_g' bands is negligibly small and the two bands cannot be detected separately, consistent with the theory for Mn oxides.[42] On the other hand, in the metallic case ($x=0.71$, 0.66, and 0.46), the relatively large chemical-potential shift indicates that the renormalization effect would be moderate and that the a_{1g} and e_g' bands can be resolved. The relationship between the quasiparticle spectral weight and the chemical-potential shift under the presence of strong electron-phonon interaction has been studied in the context of high-T_c cuprates. In the underdoped regime of $Ca_{2-x}Na_xCuO_2Cl_2$,[43] the quasiparticle spectral weight z is moderately reduced from 1 and the chemical-potential shift is given by the velocity of the quasiparticle band. While the quasiparticle spectral weight is consistent with the band velocity in the cuprates, the quasiparticle spectral weight z of the hole-doped CoO_2 plane is very small compared to the velocity of the quasiparticle band. For example, Nicolaou *et al.*[44] have shown that the quasiparticle spectral weight z is as small as 0.15 in the hole-doped CoO_2 plane while the velocity of the quasiparticle band is comparable to the prediction of the band-structure calculation. In the present study, the chemical-potential shift of the metallic region agrees with the prediction of the Hartree-Fock calculation, indicating that the relationship between the mass renormalization and the chemical-potential shift in Li_xCoO_2 is a difficult issue compared to that in the cuprates.

IV. CONCLUSION

We have performed XPS and UPS experiments on Li_xCoO_2 single crystals ($x=0.99$, 0.71, 0.66, and 0.46) which have hole-doped CoO_2 triangular lattices. The Co $2p$ XPS spectra have the charge-transfer satellite structure which is insensitive to x except the spectrum taken at 300 K for $x=0.66$ and show that the Co ion basically takes the low-spin configurations. The electronic-structure parameters such as the charge-transfer energy Δ are obtained by the cluster model analysis of the Co $2p$ core-level spectra. The valence-band UPS spectra show that the Fermi level is located near the top of the Co $3d$ t_{2g} bands and is shifted to the lower energy side with decreasing x. The fine structures near the Fermi level are consistent with the splitting of the t_{2g} band into the a_{1g} and e_g' components. The unrestricted Hartree-Fock calculation using the parameter values from the cluster-model analysis predicts that the doped holes are accommodated by the a_{1g} state up to the doping level x of 0.46. This prediction is consistent with the valence-band UPS spectra and the unrestricted Hartree-Fock calculation can describe the orbital population of the ground state. However, the line shape of the valence-band spectra cannot be reproduced by the density of states by the unrestricted Hartree-Fock calculation indicating that the correlation effect from the electron-electron and electron-phonon interactions is strong in Li_xCoO_2.

ACKNOWLEDGMENTS

The authors would like to thank A. Kakizaki and H. Takigawa for valuable comments. This work was supported in part by the Global COE Program "the Physical Sciences Frontier," MEXT, Japan.

[1] K. Mizushima, P. C. Jones, P. J. Wiseman, and J. B. Goodenough, Mater. Res. Bull. **15**, 783 (1980).
[2] E. Plichta, S. Slane, M. Uchiyama, M. Salomon, D. Chua, W. B. Ebner, and H. W. Lin, J. Electrochem. Soc. **136**, 1865 (1989).
[3] H. F. Gibbard, J. Power Sources **26**, 81 (1989).
[4] T. Nagura and K. Tazawa, Prog. Batteries Sol. Cells **9**, 20 (1990).
[5] X. Wang, I. Loa, K. Kunc, K. Syassen, and M. Amboage, Phys. Rev. B **72**, 224102 (2005).
[6] J. Molenda, C. Delmas, P. Dordor, and A. Stoklosa, Solid State Ionics **12**, 473 (1984).
[7] H. Yakabe, K. Kikuchi, I. Terasaki, Y. Sasago, and K. Uchinokura, *Proceedings of 16th International Conference on Thermoelectrics*, Dresden, 1997 (Institute of Electrical and Electronics Engineers, Piscataway, 1997), pp. 523–527.
[8] I. Terasaki, Y. Sasago, and K. Uchinokura, Phys. Rev. B **56**, R12685 (1997).
[9] K. Takada, H. Sakurai, E. Takayama-Muromachi, F. Izumi, R. A. Dilanian, and T. Sasaki, Nature (London) **422**, 53 (2003).
[10] M. L. Foo, Y. Wang, S. Watauchi, H. W. Zandbergen, T. He, R. J. Cava, and N. P. Ong, Phys. Rev. Lett. **92**, 247001 (2004).
[11] K. Miyoshi, E. Morikuni, K. Fujiwara, J. Takeuchi, and T. Hamasaki, Phys. Rev. B **69**, 132412 (2004).
[12] T. Motohashi, R. Ueda, E. Naujalis, T. Tojo, I. Terasaki, T. Atake, M. Karppinen, and H. Yamauchi, Phys. Rev. B **67**, 064406 (2003).
[13] T. Mizokawa, L. H. Tjeng, P. G. Steeneken, N. B. Brookes, I. Tsukada, T. Yamamoto, and K. Uchinokura, Phys. Rev. B **64**, 115104 (2001).
[14] T. Mizokawa, L. H. Tjeng, H.-J. Lin, C. T. Chen, R. Kitawaki, I. Terasaki, S. Lambert, and C. Michel, Phys. Rev. B **71**, 193107 (2005).
[15] M. Z. Hasan, Y. D. Chuang, D. Qian, Y. W. Li, Y. Kong, A. P. Kuprin, A. V. Fedorov, R. Kimmerling, E. Rotenberg, K. Rossnagel, Z. Hussain, H. Koh, N. S. Rogado, M. L. Foo, and R. J. Cava, Phys. Rev. Lett. **92**, 246402 (2004).
[16] H. B. Yang, S. C. Wang, A. K. P. Sekharan, H. Matsui, S. Souma, T. Sato, T. Takahashi, T. Takeuchi, J. C. Campuzano, R. Jin, B. C. Sales, D. Mandrus, Z. Wang, and H. Ding, Phys. Rev. Lett. **92**, 246403 (2004).
[17] H. B. Yang, Z. H. Pan, A. K. P. Sekharan, T. Sato, S. Souma, T. Takahashi, R. Jin, B. C. Sales, D. Mandrus, A. V. Fedorov, Z. Wang, and H. Ding, Phys. Rev. Lett. **95**, 146401 (2005).
[18] T. A. Hewston and B. Chamberland, J. Phys. Chem. Solids **48**, 97 (1987), and references cited therein.
[19] J. van Elp, J. L. Wieland, H. Eskes, P. Kuiper, G. A. Sawatzky, F. M. F. de Groot, and T. S. Turner, Phys. Rev. B **44**, 6090 (1991).
[20] M. T. Czyżyk, R. Potze, and G. A. Sawatzky, Phys. Rev. B **46**, 3729 (1992).
[21] I. Tomeno and M. Oguchi, J. Phys. Soc. Jpn. **67**, 318 (1998).
[22] M. Ménétrier, I. Saadoune, S. Levasseur, and C. Delmas, J. Mater. Chem. **9**, 1135 (1999).
[23] J. T. Hertz, Q. Huang, T. McQueen, T. Klimczuk, J. W. G. Bos, L. Viciu, and R. J. Cava, Phys. Rev. B **77**, 075119 (2008).
[24] R. E. Schaak, T. Klimczuk, M. L. Foo, and R. J. Cava, Nature (London) **424**, 527 (2003).
[25] Y. Wang, N. S. Rogado, R. J. Cava, and N. P. Ong, Nature (London) **423**, 425 (2003).
[26] J. Sugiyama, J. H. Brewer, E. J. Ansaldo, H. Itahara, T. Tani, M. Mikami, Y. Mori, T. Sasaki, S. Hébert, and A. Maignan, Phys. Rev. Lett. **92**, 017602 (2004).
[27] J. Sugiyama, J. H. Brewer, E. J. Ansaldo, B. Hitti, M. Mikami, Y. Mori, and T. Sasaki, Phys. Rev. B **69**, 214423 (2004).
[28] S. P. Bayrakci, C. Bernhard, D. P. Chen, B. Keimer, R. K. Kremer, P. Lemmens, C. T. Lin, C. Niedermayer, and J. Strempfer, Phys. Rev. B **69**, 100410(R) (2004).
[29] A. T. Boothroyd, R. Coldea, D. A. Tennant, D. Prabhakaran, L. M. Helme, and C. D. Frost, Phys. Rev. Lett. **92**, 197201 (2004).
[30] J. Sugiyama, H. Nozaki, J. H. Brewer, E. J. Ansaldo, G. D. Morris, and C. Delmas, Phys. Rev. B **72**, 144424 (2005).
[31] K. Mukai, Y. Ikedo, H. Nozaki, J. Sugiyama, K. Nishiyama, D. Andreica, A. Amato, P. L. Russo, E. J. Ansaldo, J. H. Brewer, K. H. Chow, K. Ariyoshi, and T. Ohzuku, Phys. Rev. Lett. **99**, 087601 (2007).
[32] K. Miyoshi, H. Kondo, M. Miura, C. Iwai, K. Fujiwara, and J. Takeuchi, J. Phys.: Conf. Ser. **150**, 042129 (2009).
[33] K. Miyoshi, C. Iwai, H. Kondo, M. Miura, S. Nishigori, and J. Takeuchi, Phys. Rev. B **82**, 075113 (2010).
[34] T. Mizokawa and A. Fujimori, Phys. Rev. B **54**, 5368 (1996).
[35] M. A. van Veenendaal and G. A. Sawatzky, Phys. Rev. Lett. **70**, 2459 (1993).
[36] K. Okada and A. Kotani, J. Phys. Soc. Jpn. **60**, 772 (1991).
[37] A. E. Bocquet, T. Mizokawa, T. Saitoh, H. Namatame, and A. Fujimori, Phys. Rev. B **46**, 3771 (1992).
[38] T. Saitoh, T. Mizokawa, A. Fujimori, M. Abbate, Y. Takeda, and M. Takano, Phys. Rev. B **56**, 1290 (1997).
[39] D. Qian, L. Wray, D. Hsieh, L. Viciu, R. J. Cava, J. L. Luo, D. Wu, N. L. Wang, and M. Z. Hasan, Phys. Rev. Lett. **97**, 186405 (2006).
[40] J. Geck, S. V. Borisenko, H. Berger, H. Eschrig, J. Fink, M. Knupfer, K. Koepernik, A. Koitzsch, A. A. Kordyuk, V. B. Zabolotnyy, and B. Büchner, Phys. Rev. Lett. **99**, 046403 (2007).
[41] D. J. Singh, Phys. Rev. B **61**, 13397 (2000).
[42] V. Perebeinos and P. B. Allen, Phys. Rev. Lett. **85**, 5178 (2000).
[43] K. M. Shen, F. Ronning, D. H. Lu, W. S. Lee, N. J. C. Ingle, W. Meevasana, F. Baumberger, A. Damascelli, N. P. Armitage, L. L. Miller, Y. Kohsaka, M. Azuma, M. Takano, H. Takagi, and Z.-X. Shen, Phys. Rev. Lett. **93**, 267002 (2004).
[44] A. Nicolaou, V. Brouet, M. Zacchigna, I. Vobornik, A. Tejeda, A. Taleb-Ibrahimi, P. Le Févre, F. Bertran, S. Hébert, H. Muguerra, and D. Grebille, Phys. Rev. Lett. **104**, 056403 (2010).